

DØNote 6104-CONF

## Measurement of the Mass of the Top Quark in $e\mu + \text{Jets}$ Final States at DØ with $5.3 \text{ fb}^{-1}$

The DØ Collaboration

URL <http://www-d0.fnal.gov>

(Dated: August 24, 2010)

We present a measurement of the mass of the top quark ( $m_t$ ) in  $e\mu + 2$  jets final state using data corresponding to  $5.3 \text{ fb}^{-1}$  collected by the DØ experiment at the Fermilab Tevatron. The mass is extracted from an analysis of  $t\bar{t} \rightarrow bW^+ \bar{b}W^- \rightarrow b\bar{b}e^\pm \mu^\mp \nu_e \nu_\mu$  candidate events. We employ a comparison of expected properties of the two unobserved neutrinos with the imbalance in transverse momentum in data, as a function of  $m_t$ .

We measure  $m_t = 173.3 \pm 2.4$  (stat.)  $\pm 2.1$  (syst.) GeV by combining a Run2b top quark mass measurement with  $4.3 \text{ fb}^{-1}$  and a Run2a measurement with  $1.0 \text{ fb}^{-1}$ .

*Preliminary Results for Summer 2010*

## I. INTRODUCTION

In the standard model ( $SM$ ), the masses of vector bosons are generated from spontaneous breaking of electroweak symmetry, and masses of fermions arise from their Yukawa couplings to the scalar Higgs field [1]. In  $SM$ , we can use top quark mass, and  $W$  boson mass to constraint the Higgs boson mass.

In this analysis, we measure  $m_t$  in  $e\mu$ +jets decays of  $t\bar{t}$  pairs. Each top quark decays to  $Wb$  with a branching fraction close to  $\sim 100\%$ , and each  $W$  boson decays into either a lepton and a neutrino, or two quarks. In the present analysis, we consider just those final states with one electron and one muon. They can arise from either  $W \rightarrow e(\mu)\nu$ , or from  $W \rightarrow \tau\nu \rightarrow e(\mu)\nu\nu$  decays.

The value of  $m_t$  is measured in  $4.3 \text{ fb}^{-1}$  of data collected at  $D\bar{O}$  in Run 2b of the Tevatron. The  $D\bar{O}$  detector is described in Ref. [2]. The presented analysis is based on the Neutrino Weighting method used for  $m_t$  measurement in  $1 \text{ fb}^{-1}$  of Run 2a data [3]. Assuming various top quark masses, the consistency of the observed event kinematics can be used to obtain weights for each event versus top quark mass using simulated neutrino pseudo-rapidity distributions. Weights are calculated for a range of assumed top quark masses based on the consistency of these momenta with the measured event  $\cancel{E}_T$ . We determine  $m_t$  using histograms of probability density of the first two moments of the weight distributions for different assumed  $m_t$ .

## II. SELECTION OF EVENTS

The event selection used for this measurement is similar to the one used to measure the  $t\bar{t}$  cross section in the same final state [4]. Basic requirements include one isolated electron and one isolated muon of opposite charge and transverse momenta of at least 15 GeV, exactly two jets that have transverse momenta of at least 20 GeV, and significant  $H_T$ , defined as the scalar sum of the transverse momenta of the two jets and the leading lepton. The only other requirement is that the events must pass the kinematic reconstruction of Section III. Table I shows the expected event yields for signal and backgrounds, as well as the number of events in data before and after kinematic reconstruction. The uncertainties are statistical only except for an uncertainty on signal yield, where it arises due to theoretical uncertainty on the  $t\bar{t}$  cross section. The expected yields differ from those from Ref. [4] due to a different  $H_T$  cut. For our measurement, the  $H_T$  cut was slightly increased from  $H_T > 110 \text{ GeV}$  to  $H_T > 115 \text{ GeV}$  to reduce the expected statistical uncertainty on  $m_t$ .

The signal and  $Z \rightarrow \tau\tau$  background processes are generated with ALPGEN [5], followed by PYTHIA [6] for showering and hadronization, the diboson samples (WW,WZ,ZZ) are generated with PYTHIA. Instrumental effects can cause object misidentification, and mismeasurement of missing transverse energy. Instrumental background is modeled using data.

TABLE I: Expected and observed  $e\mu$  event yield for background and signal ( $\sigma_{t\bar{t}} = 7.45 \text{ pb}$  for  $m_t = 172.5 \text{ GeV}$ ), after applying all selections. The numbers in the first six columns are given before the kinematic reconstruction.

$t\bar{t} \rightarrow e\mu$	$Z \rightarrow \tau\tau$	diboson	instrumental	total	observed	after kinematic reconstruction
$141.6^{+11.4}_{-11.4}$	$10.9^{+1.3}_{-1.3}$	$6.2^{+0.7}_{-0.7}$	$10.8^{+4.0}_{-3.8}$	$169.5^{+12.2}_{-12.2}$	202	197

## III. METHOD OF ANALYSIS

The kinematic reconstruction is based on the fact that the final state consists of the following six particles: two charged leptons, two jets from the  $b$  quarks, and two neutrinos. After the assignments of the mass to each particle in the final state, a total of 18 independent kinematic quantities needed to fully measure the final state. Twelve of these quantities – the momenta of the charged leptons and jets – are measured directly in the detector. Five additional constraints are added by requiring that

- (i) the two components of the observed imbalance in missing transverse momentum ( $\cancel{E}_T$ ) equal the sum of the respective components of the two neutrinos;
- (ii) the invariant mass of each pair of lepton and neutrino equals the  $W$  boson mass; and
- (iii) the mass of the top quark equals the mass of the antitop quark.

This leads to a total of seventeen constraints, which is one constraint short of providing a solution for the system.

A solution can be found by assuming a value of  $m_t$ . We use the measured  $\cancel{E}_T$  in each event to assign a weight to each solution. The weight is based on the agreement of the calculated transverse momentum of the neutrinos and the observed  $\cancel{E}_T$ :

$$\omega = \frac{1}{N_{\text{iter}}} \sum_{i=1}^{N_{\text{iter}}} \exp\left(\frac{-(\cancel{E}_{x,i}^{\text{calc}} - \cancel{E}_x^{\text{obs}})^2}{2\sigma_{\cancel{E}_x}^2}\right) \exp\left(\frac{-(\cancel{E}_{y,i}^{\text{calc}} - \cancel{E}_y^{\text{obs}})^2}{2\sigma_{\cancel{E}_y}^2}\right). \quad (1)$$

The calculated transverse momentum is found by ignoring the measured  $\cancel{E}_T$ , and, instead, assuming a pseudorapidity for each unobserved neutrino. From this input, the 3-momentum of each neutrino can be determined. This process is called a kinematic reconstruction.  $N_{\text{iter}}$  indicates a sum over all assignments of jets to leptons and solutions for the kinematic reconstruction. An assignment of a jet to a lepton is an assumption that both of them are final decay products of the same top quark. There are two such assumptions per event. The resolutions for the two components of  $\cancel{E}_T$ ,  $\sigma_{\cancel{E}_{x,y}}$ , are parameters of the method, and taken to be 6 GeV [3]. The top quark mass dependence on this parameter is very mild and does not create any systematic uncertainty. Integrating  $\omega$  over the the distribution in  $\eta$ ,  $\rho(\eta)$ , we obtain an overall weight  $W(m_t)$  as a function of assumed  $m_t$ :

$$W(m_t) = \int \omega(\eta_1, \eta_2) \rho(\eta_1) \rho(\eta_2) d\eta_1 d\eta_2. \quad (2)$$

The distributions in neutrino pseudorapidity are all modeled as Gaussians, with root-mean-square (rms) of 1.0.

To kinematically reconstruct an event, we have to solve a system of two quadratic equations. If none of the solutions have real values, the event is said to fail kinematic reconstruction. The breakdown in efficiencies for kinematic reconstruction for different event sources is given in Table II. The efficiencies are defined as the ratio of expected event yield before the reconstruction and the yield after the reconstruction.

TABLE II: Efficiencies for kinematic reconstruction of events, with  $H_T > 115$  GeV cut.

sample	$t\bar{t}$ (172.5 GeV)	$Z \rightarrow \tau\tau$	diboson	data
efficiency,%	$98.7 \pm 0.05$	$96.6 \pm 2.3$	$92.3 \pm 2.4$	$97.5 \pm 1.1$

Weights calculated for different  $m_t$  yield a weight distribution for each event, which depends significantly on the number of sampling points used for each neutrino pseudorapidity distribution. In previous versions of this analysis, we used 10 sampling points. We have tested the analysis using 10 to 200 sampling points of neutrino  $\eta$ , and find that 29 such points ensure the optimal performance of the method. This sampling results in the desired gain in kinematic reconstruction efficiency and statistical uncertainty on  $m_t$  while balancing against CPU requirements. The overall weight  $W(m_t)$  is calculated in 1 GeV increments for  $80 < m_t < 330$  GeV by summing over all the weights for each chosen neutrino  $\eta$ .

#### IV. PROBABILITY DENSITY HISTOGRAMS

For each event,  $W(m_t)$  is obtained as a function of the assumed  $m_t$ . Two parameters are chosen to characterize this distribution for every event [3], namely the mean ( $\mu_w$ ) and root-mean-square ( $\sigma_w$ ) of the distribution. The normalized three-dimensional distribution of  $\mu_w$ ,  $\sigma_w$ , and input  $m_t$  yields a signal probability histogram,  $h_s(\mu_w, \sigma_w, m_t)$ . The background probability density histogram,  $h_b(\mu_w, \sigma_w)$  which is not a function of  $m_t$ , is obtained as the two-dimensional distribution of  $\mu_w$  and  $\sigma_w$  of simulated background events. Weights are assigned to events of different background sources that correspond to their relative contributions. Probability density histograms scaled to expected event yields for background  $h_b(\mu_w, \sigma_w)$  and signal  $h_s(\mu_w, \sigma_w, 175 \text{ GeV})$ , and dependence of  $\mu_w$  on  $m_t$  for  $25 < \sigma_w < 35$  are shown in Fig. 1.

#### V. MAXIMUM LIKELIHOOD

After having modeled the signal probability histogram,  $h_s(\mu_w, \sigma_w | m_t)$ , and background probability density histogram,  $h_b(\mu_w, \sigma_w)$ , the top quark mass is extracted by maximizing the likelihood:

$$\mathcal{L}(\mu_{\omega\{1..N\}}, \sigma_{\omega\{1..N\}}, N | \bar{n}_b, \bar{n}_s | m_t) = \prod_{i=1}^N \frac{\bar{n}_s h_s(\mu_{\omega_i}, \sigma_{\omega_i} | m_t) + \bar{n}_b h_b(\mu_{\omega_i}, \sigma_{\omega_i})}{\bar{n}_s + \bar{n}_b}. \quad (3)$$

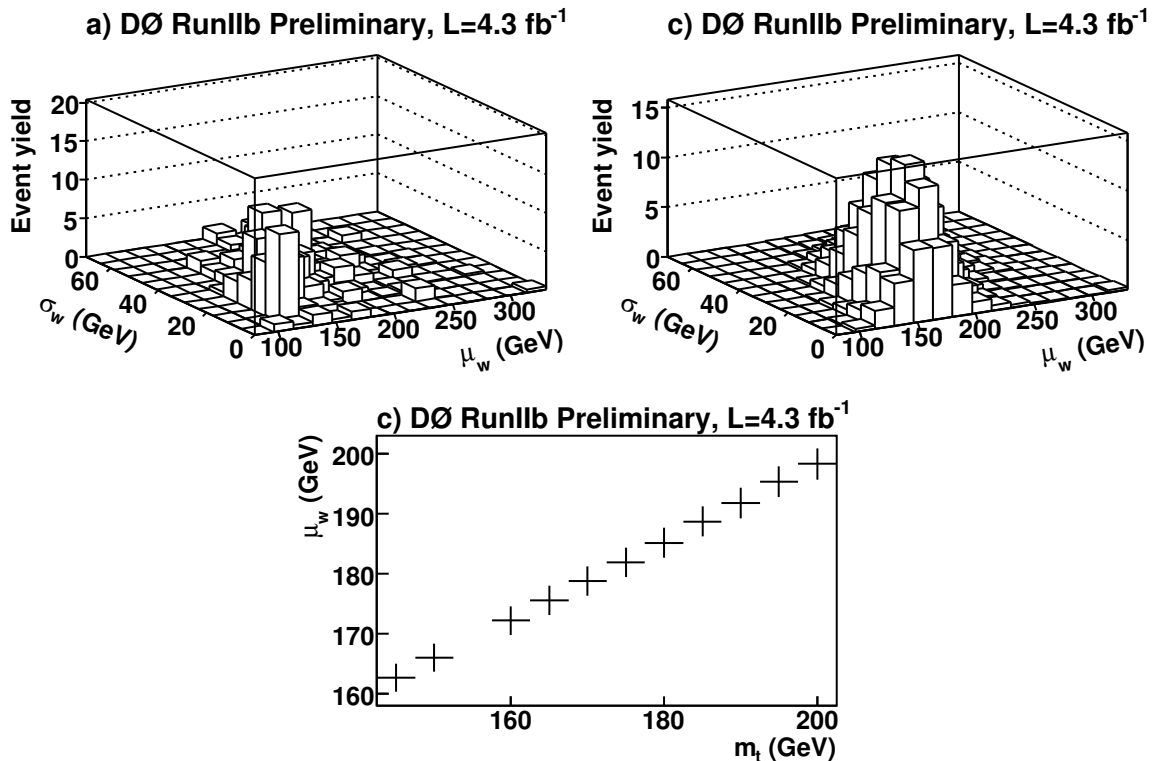


FIG. 1: The calculated probability density histogram scaled to expected event yields for (a) background, (b) signal with  $m_t = 175$  GeV as a function of  $\mu_w$  and  $\sigma_w$ , and (c) dependence of  $\mu_w$  on  $m_t$  for signal.

Here  $\bar{n}_s$  and  $\bar{n}_b$  are the expected event yields for signal and background respectively, and  $N$  is the total number of selected events. The parameters of the likelihood are broken into three groups: measured, expected, and fitted parameters. Uncertainties on the likelihood appear due to the finite statistics in our signal Monte Carlo samples. The distribution of  $-\log \mathcal{L}$  vs.  $m_t$  is fit by a parabola taking into account generated top mass values within an interval of  $\pm 15$  GeV around the likelihood point with the lowest value. The value of  $m_t$  at the minimum of the parabola defines our top quark mass estimate,  $\hat{m}_t$ . Half the width of the parabola where  $-\log \mathcal{L}$  rises to 0.5 units more than its minimum value provides the statistical uncertainty,  $\hat{\sigma}_{m_t}$ .

The performance of the mass extraction technique is evaluated using ensemble testing techniques: the top quark mass  $m_t$  is extracted in ensembles of pseudoexperiments of 197 events. The events are chosen randomly from the signal and background Monte Carlo samples so that the average number of background events per source matches the expected yield. The actual number of events in a given pseudoexperiment is obtained according to a Poisson distribution. The mean of the Poisson distribution is taken from a Gaussian distribution centered at the expected event yield and with uncertainty equal to the total statistical uncertainty.

We employ two approaches for the ensemble tests. In the first approach, which is used for the measurement, we use the information about signal cross section from theory in Table I for all mass points. We fluctuate signal in the same way as the background processes and we select only those pseudoexperiments for which the total number of events exactly equals those observed in data. We employ 1000 pseudoexperiments in an ensemble, and we correct for the correlations among pseudoexperiments since the events are used in the pseudoexperiments more than once. However, the expected signal cross section may not accurately reflect the actual number of  $t\bar{t}$  events in the selected sample. Consequently, the number of  $t\bar{t}$  used for the ensemble tests can be incorrect. Also, this number depends on the assumed  $m_t$ . This might lead to a bias in the calibration of measured  $m_t$ . Therefore, we use a second approach [3] as a cross-check. We give up the information on the expected cross section, and the signal event yield in a pseudoexperiment is taken as the number of data events minus the total background event yield. Both approaches give consistent results.

Figure 2 shows a good agreement between the output and input top quark mass for the first approach and demonstrates the validity of the statistical error estimation, with widths of pull distributions near their expected value of 1.0. The linear fits in Fig. 2 are used to calibrate the results from data, mapping the output minimum to an input top quark mass. The results of the fits are summarized in Table III. The neutrino pseudorapidity distribution is mass

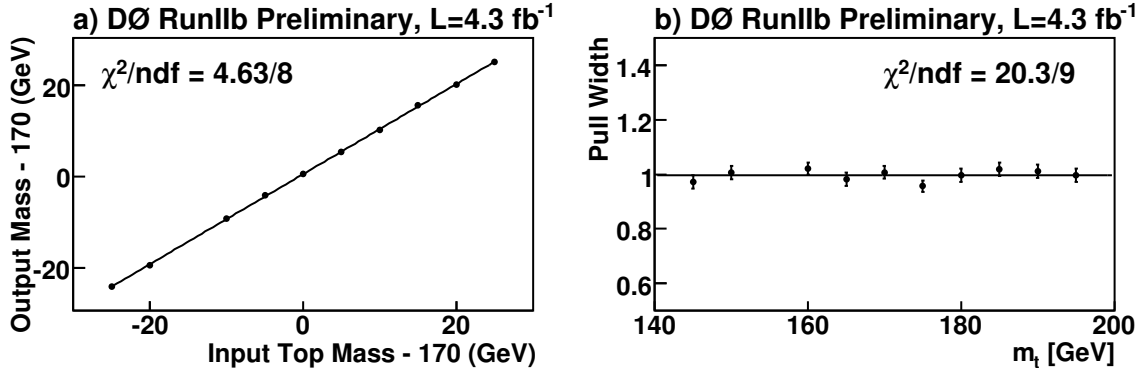


FIG. 2: (a) shows the fitted top quark mass as a function of the generated MC input top quark mass with central value of the signal cross section taken from theory and with a correction for resampling MC events, and (b) pull width distributions with the same treatment.

dependent, and our analysis assumes a mass-independent Gaussian of width 1.0. We tested the sensitivity of our analysis to this choice by repeating the analysis with a mass-dependent width fit in MC top samples with generator masses of 130 GeV to 210 GeV. The estimated expected statistical uncertainty changed by only 0.03 GeV. We also checked the stability of the result for variations in the range used in the fit, and the small dependence of the minimum on the width of the window for the fit is included in the calibration uncertainty on the final result.

	slope	offset (GeV)	$\langle$ pull width $\rangle$
signal cross section from theory	$0.99 \pm 0.006$	$0.45 \pm 0.09$	$1.0 \pm 0.007$

TABLE III: Slope and offset of the calibration curve in Fig. 2, and the pull width.

## VI. RESULTS

The top quark mass is estimated by maximizing the likelihood for the selected data. The top quark mass estimate and uncertainties are corrected to account for the calibration from ensemble tests (slope and offset, and pull widths) by using the calibration curves of Fig. 2. The measured top quark mass after calibration yields  $m_t = 172.73 \pm 2.81$  (stat.) GeV. The cross-check measurement is within 0.1 GeV of this result.

The negative log likelihood as a function of top quark mass before the calibration, together with the parabolic fit, are shown in Fig. 3. The distribution of expected statistical uncertainties is shown in Fig. 4, overlaid with the value observed in data.

## VII. SYSTEMATIC UNCERTAINTIES

A summary of the systematic uncertainties is given below.

- (i) *Jet energy scale*: We evaluate this systematic uncertainty by shifting the jet energy scale by  $+\sigma$  and  $-\sigma$  and symmetrizing the errors. This uncertainty is found to be 1.35 GeV.
- (ii) *b/light jet response*: The calorimeter response is different for the light quark and  $b$ - jets. To estimate this difference, particle jets in a  $t\bar{t} l$ +jets sample were classified as  $b$ - or light quark jets. Single particle response curves for both data and MC were then applied to the particle jets to predict the energy of a reconstructed jet in the calorimeter. The double ratio of jet transverse momenta in data and MC is estimated to be 1.8%. We found the  $b$ /light jet response systematic uncertainty by shifting the response down by 1.8% and remeasuring the top quark mass. We symmetrize this error and assign a systematic uncertainty of  $\pm 0.8$  GeV.

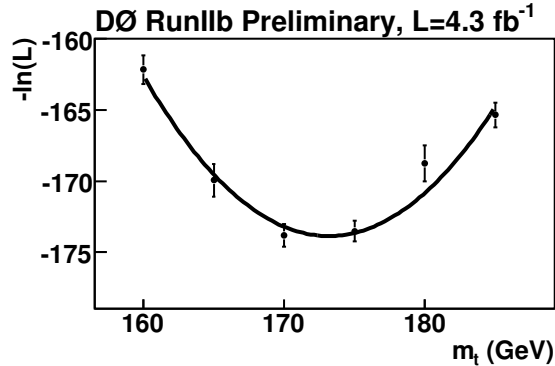


FIG. 3: Negative log likelihood distribution for data before calibration.

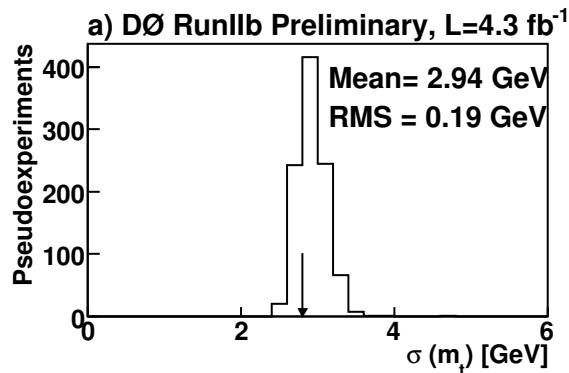


FIG. 4: Distribution of statistical uncertainties after correcting for the pull width and slope for  $m_t^{\text{MC}}=170$  GeV. Arrow indicates the measured statistical uncertainty on  $m_t$ .

- (iii) *Jet resolution*: The jet resolution in Monte Carlo is smaller than in data. Therefore, an additional oversmearing is applied to the simulated jets. This additional oversmearing has some uncertainty. We evaluate the jet energy resolution by shifting the jet resolution by  $+1\sigma$  and  $-1\sigma$  and symmetrizing the errors. This systematic uncertainty is found to be 0.4 GeV.
- (iv) *Calibration uncertainty*: The calibration uncertainty arises from the errors on the offset and slope of calibration curve. Using error propagation, we get an uncertainty of 0.1 GeV for the top quark mass.
- (v) *Template statistics*: The templates have finite statistics. Local fluctuations in these templates can cause local fluctuations in the individual likelihood fits and the top quark mass. We obtain an uncertainty in  $m_t$  by varying the results of the negative likelihood fits from the data ensemble within their errors and repeating the fit to the distribution. The width of the  $m_t$  distribution provides the systematic uncertainty. It is found to be 0.35 GeV.
- (vi) *Initial state radiation (ISR) and final state radiation (FSR)*: We evaluate this systematic uncertainty by comparing Pythia with ISR and FSR parameters varied up and down [7]. After symmetrization of errors, we found this to be 0.55 GeV.
- (vii) *Hadronization and underlying events*: We evaluate this systematic uncertainty by comparing ALPGEN + PYTHIA with HERWIG [8]. We conclude that hadronization and underlying event systematic uncertainty is 0.3 GeV.
- (viii) *Color reconnection*: We evaluate this by comparing PYTHIA tuneACRpro [9] and tuneApr [10]. The uncertainty is found to be 0.7 GeV.
- (ix) *Higher order effects*: We evaluate this systematic uncertainty [9] by comparing ALPGEN + PYTHIA with MC@NLO [11] + HERWIG. This is found to be 0.2 GeV.

Source	Uncertainty (GeV)		
	4.3 fb <sup>-1</sup>	1 fb <sup>-1</sup>	combination
Statistical	±2.8	±4.4	±2.4
Jet energy scale	±1.35	±1.4	±1.4
<i>b</i> -jet energy scale	±0.8	±0.5	±0.7
Jet resolution	±0.4	±0.2	±0.3
Signal fraction	0	±0.1	0
Calibration uncertainty	±0.1	±0.1	±0.1
Template statistics	±0.35	±0.7	±0.3
ISR/FSR	±0.55	±0.2	±0.45
Hadronization and UE	±0.3	±0.7	±0.4
Color reconnection	±0.7	±0.7*	±0.7
Higher order effects	±0.2	±0.2*	±0.2
<i>b</i> fragmentation	±0.4	±0.4	±0.4
Background shape	±0.3	±0.3	±0.3
Sample dependent	0	±0.2	±0.2
Muon/track <i>p<sub>T</sub></i> resolution	±0.2	±0.2	±0.2
Electron energy resolution	±0.2	±0.2	±0.2
Jet identification	±0.5	±0.5	±0.5
Total systematic uncertainty	±2.1	±2.1	±2.1

TABLE IV: Summary of uncertainties for the Run 2b analysis, the Run2a analysis, and their combination. Run 2a systematic uncertainties marked with \* are taken from Run 2b.

A list of all evaluated systematic uncertainties is shown in Table IV. The systematic uncertainties are dominated by jet energy scale uncertainties. The combined systematic uncertainty is  $\pm 2.1$  GeV.

### VIII. COMBINATION WITH THE RUN 2A DILEPTON TOP QUARK MASS MEASUREMENT.

The DØ Collaboration has published a measurement in the dilepton channel [3] using data corresponding to an integrated luminosity of 1 fb<sup>-1</sup> from Run 2a yielding  $m_t = 174.7 \pm 4.4$  (stat.)  $\pm 2.0$  (syst.) GeV. This sample is statistically uncorrelated with the sample discussed in this note. The systematic uncertainties for MC calibration and template statistics are also uncorrelated between the two measurements. All other systematic uncertainties are taken to be 100% correlated. We do not assign a sample dependent systematic uncertainty in Run 2b because of improved simulation. Color reconnection and higher order effects systematics have been estimated for the current measurement, but not for the earlier one. We have applied the newer results to the older data. Combining the two measurements [12] and accounting for correlations between uncertainties, we obtain  $m_t = 173.3 \pm 2.4$  (stat.)  $\pm 2.1$  (syst.) GeV.

### IX. CONCLUSION

In proton-antiproton collision data corresponding to an integrated luminosity of 5.3 fb<sup>-1</sup>, we have used the neutrino weighting method to measure a top quark mass from  $t\bar{t}$  events in  $e\mu$  final state. We measured the top quark mass to be:

$$m_t = 173.3 \pm 2.4 \text{ (stat.)} \pm 2.1 \text{ (syst.) GeV,}$$

by combining the Run2b 4.3 fb<sup>-1</sup> result

$$m_t = 172.7 \pm 2.8 \text{ (stat.)} \pm 2.1 \text{ (syst.) GeV}$$

with the Run2a 1.0 fb<sup>-1</sup> [3] result

$$m_t = 173.3 \pm 2.4 \text{ (stat.)} \pm 2.1 \text{ (syst.) GeV.}$$

This is the most precise single measurement in the dilepton channel.

---

- [1] W. Marciano, arXiv:hep-ph/0411179 (2004).
- [2] V.M. Abazov, *et al.*, Nucl. Instrum. Methods in Phys. Res. Sect. A **565**, 463 (2006).
- [3] V.M. Abazov, *et al.*, “Measurement of the top quark mass in final states with two leptons,” Phys. Rev. D **80**, 092006 (2009).
- [4] The D0 Collaboration, “Measurement of the  $t\bar{t}$  Production Cross-Section in Dilepton Final States at D0 using  $5.3^{-1}$  fb of Data,” D0 Note 6038-CONF, (2010).
- [5] M.L. Mangano, *et al.*, “ALPGEN, a generator for hard multiparton processes in hadronic collisions,” J. High Energy Physics **0307**, 001 (2003).
- [6] T. Sjöstrand, L. Lönnblad, and S. Mrenna, “PYTHIA 6.2 Physics and Manual,”.
- [7] CDF Note 6804, [http://hep.uchicago.edu/~hslee/ISR/cdf6804\\_ISR\\_DY.ps](http://hep.uchicago.edu/~hslee/ISR/cdf6804_ISR_DY.ps).
- [8] G. Corcella *et al.*, J. High Energy Physics **0101**, 010 (2001).
- [9] A. Buckley *et al.*, Eur. Phys. J. C **65**, 331 (2010).
- [10] R. Field and R. C. Group [CDF Collaboration].
- [11] S. Frixione and B. Webber, J. High Energy Physics **06**, 029 (2002).
- [12] L. Lyons, D. Gibaut, and P. Clifford, Nucl. Instrum. Methods Phys. Res. A **270**, 110 (1988); A. Valassi, Nucl. Instrum. Methods Phys. Res. A **500**, 391 (2003).